International Journal for Housing Science and Its Applications
Publish August 10, 2025. Volume 46, Issue 4 Pages 4593-4606

https://doi.org/10.70517/ijhsa464303

Design and Practical Exploration of Simulation Teaching Model for Dynamic Behavior of Structural Seismic Resistance Combined with Finite Element Methods

Yujing Xiong[1,*]
[1] College of Intelligent Construction, Hunan Software Vocational and Technical University, Xiangtan, Hunan, 411100, China
Corresponding authors: (e-mail: xiongyujing1988@163.com).

Abstract With the increasing requirements for seismic performance of building structures, the seismic design of reinforced concrete structures is particularly important. In this study, the dynamic elastic-plastic analysis of reinforced concrete frame structures was carried out using ABAQUS finite element software to investigate the effects of different bracing forms on the seismic performance of the structures. An explicit dynamic analysis method was adopted to analyze the time-dependent response of 5-story and 10-story frame structures using El Centro seismic waves and Kyushu 3D Kumamoto seismic waves in Japan as input loads. It was found that the frame with herringbone bracing had the greatest lateral stiffness under the 9-degree seismic action, reaching four times that of the pure frame, while the frames with cross-bracing and V-bracing had lateral stiffnesses that were 2.6 and 2.3 times that of the pure frame, respectively. In addition, the analysis shows that the maximum floor displacements range from -300 mm to 200 mm for 5-story frames and from -400 mm to 500 mm for 10-story frames, showing good seismic performance. The maximum storey displacements were 76mm and 60mm respectively, which were less than the angular limit of plastic storey displacement of 0.02. The results of the study show that different forms of center bracing can significantly improve the seismic performance of the frames.

Index Terms Reinforced concrete structure, finite element analysis, seismic performance, ABAQUS, time response, seismic waves

I. Introduction

The seismic course of engineering structures is an important professional course in the upper-division undergraduate curriculum of civil engineering majors, and its pre-requisite courses need to complete the mechanics class, foundation foundation, steel structure and concrete structure design principles and other courses [1], [2]. The course integrates the professional knowledge of each course, covers a wide range of professional knowledge points, closely follows the engineering practice and specifications, which not only synthesizes the content of the previous courses, but also lays the foundation for the subsequent graduation design and postgraduate studies [3], [4]. Therefore, the course has become one of the most important professional courses in the senior curriculum, which puts high requirements on teachers and students, not only requiring students to master the professional knowledge points in the pre-requisite courses, but also requiring lecturers to master the latest research results at home and abroad [5], [6].

However, the previous course formative assessment results in the classroom quizzes and post-course assignments are used in the assessment method, students only focus on the content of the books, and even rote memorization is not well understood, it is difficult to realize the cultivation of high-quality talents [7], [8]. In order to enable students to combine book content and practice, and improve students' perceptual knowledge of seismic structural design, it is necessary to reform the traditional teaching and course assessment methods, and by combining the finite element method can effectively improve the teaching effect of seismic teaching in colleges and universities [9]-[11]. Finite element method is a numerical calculation method for solving mathematical equations, which is a numerical analysis technology that organically combines theory, calculation and computer software [12], [13]. In the teaching of structural seismic resistance, the finite element method can realize the seamless connection between theoretical derivation and engineering practice, which meets the course teaching demand of simulation of dynamic behavior of structural seismic resistance, and is of great significance for improving the quality of course teaching [14]-[16].

In this paper, the dynamic elastic-plastic analysis of reinforced concrete frame structures will be carried out by using ABAQUS, focusing on the effect of different bracing forms on the seismic performance of the structure. Firstly,

by modeling the frame with different bracing forms, the dynamic analysis is performed and the response of the structure is solved. Secondly, the seismic performance of various types of frames, especially their deformation, displacement and stiffness degradation under seismic loading, is evaluated by combining with time-course analysis. Finally, through comparative analysis, the role of different bracing methods in enhancing the seismic performance of the structure is explored to provide a theoretical basis for the seismic design of the building.

II. ABAQUS elasto-plasticity analysis parameter calculation and model building

In this paper, dynamic elasto-plastic analysis will be carried out using ABAQUS.

II. A.Finite element theory

The methods of computer numerical simulation include the finite element method, the infinite element method and the finite volume method. At present, the finite element method is more widely used, and its basic principle is to replace the continuous solution domain, by means of discretization, with a set of units of the assemblage, and the approximation function set in each unit is used to represent the unknown field function to be solved on the solution domain. The approximation function is generally expressed in terms of the unknown field function, so that a continuous infinite-degree-of-freedom problem becomes a discrete finite-degree-of-freedom problem.

The solution process:

Step1: Discretization of the structure.

Step2: Solve for each cell stiffness matrix $\left[K^e\right]$.

Step3: Integrate the overall stiffness matrix $\left[K\right]$ and list the overall equilibrium equation.

Step4: Introduce boundary conditions to find out each node displacement.

Step5: Solve for the stress and strain of each unit.

II. B.ABAQUS finite element analysis

II. B. 1) General

ABAQUS finite element software is commonly used in research simulation because of its outstanding nonlinear analysis performance and wide applicability. ABAQUS provides ABAQUS/CAE visualization work module, which allows easy and fast modeling, submitting and monitoring of jobs, and powerful post-processing functions [17].

ABAQUS analysis module mainly consists of ABAQUS/Standard implicit module and ABAQUS/Explicit explicit module, and also contains some additional analysis modules.

The ABAQUS/Standard module is widely used and provides a very rich set of material models for solving linear and nonlinear problems in a large number of research areas.

ABAQUS/Explicit is mainly used for solving transient dynamic problems and problems with a high degree of nonlinearity, and one of its major advantages is that it occupies little disk space and memory, so the computational cost is small. ABAQUS not only provides itself with a very rich material and unit models, but also provides a large number of interfaces for the user-written subroutines, such as customized material models, to meet the user's individual needs.

II. B. 2) Types of Finite Element Models for Reinforced Concrete Structures

Finite element modeling of reinforced concrete structures does not differ much from the general solid modeling approach, but two points should be considered:

(1) The material intrinsic modeling of reinforced concrete is more complex, e.g., the inhomogeneity of the concrete material and the tensile and compressive properties of concrete vary greatly.

(2) Since the reinforced concrete structure is composed of two different materials, the finite element is characterized by discretization, such as bond slip between reinforced concrete.

The finite element model of reinforced concrete structure is mainly divided into: monolithic, discrete and combined.

Integral models mainly simulate the macroscopic response of the structure under loading, and can be used to calculate the approximate stress-strain changes of the structure as a whole. This type of model is usually used for rough simulation of the structure, but it can also be used for rough simulation of the structure when limited by the performance of the computer. It is common practice to diffuse the reinforcement into the concrete to account for the contribution of the reinforcement to the structure, which is then considered to be composed of a single homogeneous material. In the analytical model in this chapter, a monolithic model was used to diffuse the hoop reinforcement in the structure into the concrete.

Separate model according to the reinforcement and concrete, respectively, to select their respective unit types and material structure for modeling, can fully consider the mechanical properties of the reinforcement and concrete, so that the established finite element model is more accurate, close to the actual situation.

The advantage of the separated model over the combined and monolithic models is that the bond-slip between reinforcing steel and concrete can be simulated by inserting the linkage unit. However, at the same time, there will be a problem, that is, the division of reinforcing steel unit is too coarse to achieve the desired simulation effect, while the division of reinforcing steel unit is too fine will lead to the interface between the reinforcement and the concrete there will be a lot of transition units, the need to set up a large number of linkage units at the common node, appropriate reduction in the number of division of reinforcing steel unit can be achieved by the simulation of the concrete structure of the local components, but it is difficult to realize the overall structure of the concrete simulation and analysis of the finite element model. Analysis.

The modeling difficulty and simulation accuracy of the combined model are higher than that of the integral model and lower than that of the separated model, which is relatively simple and can get better simulation results. The combined model considers that there is no relative slip between the reinforced concrete and the reinforcing steel, and the composite unit stiffness matrix is formed by superimposing the effects of reinforcing steel and concrete on the unit stiffness matrix to reflect the joint work of reinforcing steel and concrete. The reinforced concrete composite unit is used for modeling in this chapter.

II. C.ABAQUS-based modeling approach

(1) Preprocessing

The pre-processing module includes the sub-modules of parts, properties, assembly, analysis step, interaction, load, mesh and analysis job.

Components are the basic elements of an ABAQUS model, including geometric components and mesh components.

The main role of properties is to define the ontological relationships of the components of the model being built. Defining material properties in ABAQUS is generally divided into three steps: inputting the principal model of the components, defining the structural or component cross-section properties, and assigning the defined cross-section properties to the corresponding components. Assembly is the positioning and assembling of components to form an assembly.

There are four operations in the analysis step: creating the analysis step, setting the output data, setting the adaptive mesh and controlling the analysis.

The Interaction module serves to define the contacts and constraints between entities.

Loads provides a large number of loading methods, including the more common types of loads in real engineering, such as: concentrated load, moment load, pressure load, surface load, body load, line load and gravity load.

The essence of Finite Element Analysis (FEA) is to convert a problem with infinite degrees of freedom into a problem with finite degrees of freedom, and to convert a continuous model into a discrete model for analysis. The mesh module is meant to discretize the model.

The job includes functions such as creating and editing jobs, submitting jobs, generating INP files, job monitoring and interrupting jobs.

(2) Post-processing

The essence of post-processing is to check and process the calculation results, including checking the stress and strain, and plotting the load and displacement curves.

(3) Solving method

ABAQUS includes two modules of implicit static and display dynamic solution.

II. D.Ontological relationships of materials

In the finite element numerical analysis, the reasonable or not of the mechanical properties of the structural constituent materials has a significant impact on the results of the analysis and calculation. Especially in the reinforced concrete finite element model, the ontological relationship of concrete has a significant impact on the nonlinear analysis of the overall structure. In continuum mechanics, there are more modeling theories about the ontological relationship of deformed bodies, such as elasticity theory, nonlinear elasticity theory, viscoelasticity, viscoplasticity theory, elasto-plasticity theory, damage mechanics theory and so on.

II. D. 1) Intrinsic Relationships of Reinforcing Steel

Compared to concrete, the mechanical properties of reinforcing materials are simpler and clearer.

Based on the stress-strain relationship curves of soft and hard steel during monotonic loading. The most common elastic-plastic principal constitutive models are:

(1) Ideal elastic-plastic bilinear model: the elastic phase of the eigenstructure curve is an oblique straight line, and after yielding by force, it is a horizontal straight line, and the stress no longer increases.

(2) Elasticity-ideal plasticity-hardening plastic model: this constitutive relationship that the steel bar after yielding through a yielding platform and then enter the strengthening stage.

(3) Reinforcement bifurcation model: there is no descending section in the curve of this constitutive relationship, and the elastic modulus of the bar is the slope of the first ascending section of the bifurcation line, which enters into the second ascending section, i.e., the reinforcing stage, after yielding. The slope can be about 1/100 of the initial elastic modulus.

In this paper, the ideal elastic-plastic bilinear principal relationship model is adopted, and the principal equation is shown in equation (1):

$$\sigma_s = \begin{cases} E_s \varepsilon_s & \varepsilon_s \le \varepsilon_y \\ f_y & \varepsilon_s > \varepsilon_y \end{cases} \tag{1}$$

where σ_s is the stress of the reinforcement and ε_s is the strain of the reinforcement. ε_y is the yield stress of the reinforcement. ε_y is the yield strain of the reinforcement.

II. D. 2) Intrinsic relationships of concrete

The stress-strain curve for uniaxial compression is shown in Fig. 1.

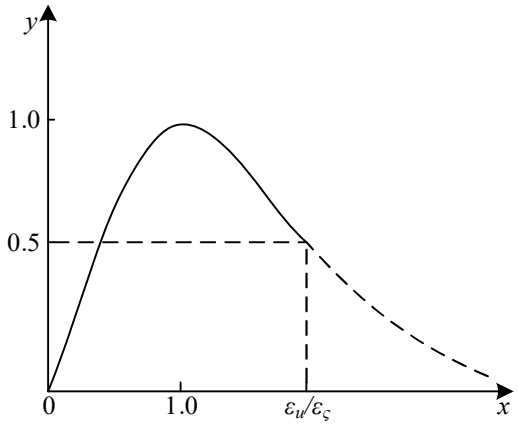

Figure 1: Constitutive relations of Sargin

This stress-strain principal curve equation is expressed by the following equation:

$$\sigma = (1 - d_c) E_c \varepsilon \tag{2}$$

$$d_c = \begin{cases} 1 - \dfrac{\rho_c n}{n - 1 + x^n} & x \le 1 \\ 1 - \dfrac{\rho_c}{\alpha_c (x-1)^2 + x} & x > 1 \end{cases} \tag{3}$$

$$\rho_c = \frac{f_{c,r}}{E_c \varepsilon_{c,r}} \tag{4}$$

$$n = \frac{E_c \varepsilon_{c,r}}{E_c \varepsilon_{c,r} - f_{c,r}} \tag{5}$$

$$x = \frac{\varepsilon}{\varepsilon_{c,r}} \tag{6}$$

where α_c is the parameter value of the descending section of the uniaxial compressive stress-strain curve of concrete. $f_{c,r}$ is the representative value of uniaxial compressive strength of concrete. $\varepsilon_{c,r}$ is the peak

compressive strain of concrete corresponding to the representative value of uniaxial compressive strength. d_c is the uniaxial compressive damage evolution coefficient of concrete.

The tensile stress-strain principal relationship for concrete in this paper is based on the principal relationship specified in the code for the design of concrete structures, with appropriate simplifications.

The equation for this stress-strain curve can be determined from the following series of equations:

$$\sigma = (1-d_t)E_c\varepsilon \tag{7}$$

$$d_t = \begin{cases} 1-\rho_t[1.2-0.2x^5], & x \le 1 \\ 1-\dfrac{\rho_t}{\alpha_t(x-1)^{1.7}+x}, & x > 1 \end{cases} \tag{8}$$

$$x = \frac{\varepsilon}{\varepsilon_{t,r}} \tag{9}$$

$$\rho_t = \frac{f_{t,r}}{E_c\varepsilon_{t,r}} \tag{10}$$

where α_t is the parameter value of the descending section of the uniaxial tensile stress-strain curve of concrete. $f_{t,r}$ is the representative value of uniaxial tensile strength of concrete. $\varepsilon_{t,r}$ is the peak tensile strain of concrete corresponding to the representative value of uniaxial tensile strength. d_c is the uniaxial tensile damage evolution coefficient of concrete.

II. E. Basic Theory of Seismic Performance Analysis

(1) Hysteresis curve

The hysteresis curve, also known as the restoring force characteristic curve, is a curve that indicates the change of restoring force with deformation. The hysteresis curve reflects the deformation characteristics, stiffness degradation and energy consumption of the structure during repeated loading, and is the basis for determining the restoring force model and nonlinear seismic response analysis. In structural seismic analysis, repeated static load tests are often used to determine the hysteresis curve. The structure will deform accordingly with the application of the load under the horizontal low circumferential reciprocating load, and a force and displacement curve will be generated after every cyclic loading, and the hysteresis curve is a combination of multiple hysteresis loops. Typical shapes of hysteresis curves are mainly categorized into: shuttle, bow, inverse S-shape and Z-shape [18].

(2) Skeleton curve refers to the envelope curve obtained by connecting the load extreme points of each loading in the same direction (tension or compression) on the hysteresis curve. The skeleton curve is the trajectory of the maximum peak value of the force reached by repeated cyclic loading in the low week, reflecting the important characteristics of the force and deformation of the member at different stages, such as member strength, stiffness, ductility, energy consumption and collapse resistance, which can visually represent the deformation and bearing capacity of the member under the action of the load.

(3) Stiffness degradation

Structures or components in the horizontal repeated loads, with the reciprocal loading, the load reaches the same peak point when the structure or component displacement and deformation of the phenomenon known as stiffness degradation. Component in the loading process will go through the linear elastic stage, strengthening stage and strength degradation stage, in the strengthening stage of the structure or component of the load capacity increase is no longer linear, which is due to the accumulation of internal damage caused by the material, and at the same time, the stiffness of the component will produce degradation. Stiffness degradation can be visualized in the form of structural or component cracks appear, carry out and deformation development process, the standard stiffness degradation curve contains rapid degradation section, sub-degradation section and slow degradation section, the stiffness decay characteristics and degradation rate can be used to measure the seismic performance of the structure or component, through the stiffness degradation curve can be intuitively reacted to the stiffness degradation of the component in the process of loading.

(4) Ductility

The damage forms presented by members under seismic loading include brittle damage and ductile damage. After the member reaches the ultimate bearing capacity, the deformation continues for a period of time, and the signs before damage are obvious. The structural design should ensure that the damage form of the member under seismic force favors ductile rather than brittle.

(5) Energy dissipation capacity

Energy-consuming capacity refers to the ability of the member to release energy into heat by internal damage of the material when subjected to repeated loads, which is manifested in the ability of the member to absorb energy by plastic deformation. The measure of energy dissipation capacity of the member can refer to the cumulative energy consumption, energy consumption coefficient and equivalent viscous damping coefficient.

II. F. Equations for dynamic time-dependent analysis

Dynamic elastic-plastic analysis is one of the important achievements in the development of structural analysis technology, and it is an important part of the research and analysis method of seismic performance of structures. Dynamic elastic-plastic analysis method is to analyze the structure as an elastic-plastic vibration system, and directly input the ground motion according to the seismic wave data, and through the integral operation, find out the internal force and deformation of the structure in the acceleration of the ground with the change of time, the whole process of the structural change of the internal force and deformation of the structure with the change of time. The seismic wave responds to the whole process of the earthquake, and the elastic-plastic time-course analysis can truly reflect the structural response at each moment under the action of the earthquake, including the deformation, stress, and damage pattern (cracking and destruction), and so on. The structural response under an earthquake is nonlinear, not only the structural material enters the elastic-plastic working state, the strength and stiffness degradation occurs or reaches structural damage, in which the geometric nonlinear effect caused by the overall lateral movement of the structure is also more significant.

Dynamic equilibrium equations of the structure:

$$M\ddot{U} + C\dot{U} + K\ddot{U} = R \tag{11}$$

where M is the mass matrix of the system. C is the damping matrix of the system. K is the stiffness matrix of the system. $\ddot{U}$ is the acceleration vector. $\dot{U}$ is the velocity vector. U is the displacement vector. R is the external load vector.

In general, for solving the above equilibrium equations, there are vibration mode decomposition method and direct integration method. The direct integration method is divided into two categories: explicit and implicit algorithms. In this paper, the implicit algorithm is chosen for the dynamic elastic-plastic analysis of the structure, and the two included algorithms, $Wilson-\theta$ method and $Newmark-\beta$ method, are described respectively.

(1) $Wilson-\theta$ method: it is essentially a generalization of the linear acceleration method, which assumes that the acceleration varies linearly from moment t to moment $t+\Delta t$. The $Wilson-\theta$ method assumes that the acceleration varies linearly from moment t to moment $t+\theta\Delta t$, where $\theta \geq 1.0$. When $\theta = 1.0$, the method reduces to a linear acceleration format. To achieve unconditional stabilization, $\theta \geq 1.37$ must be made.

Let τ denote the time increment $(0 \leq \tau \leq \theta\Delta t)$, then for the time interval from t to $t+\theta\Delta t$, assume:

$$\ddot{U}_{t+\tau} = \ddot{U}_t + \frac{\tau}{\theta\Delta t}(\ddot{U}_{t+\theta\Delta t} - \ddot{U}_t) \tag{12}$$

Integrating the above equation yields:

$$\dot{U}_{t+\tau} = \dot{U}_t + \ddot{U}_t\tau + \frac{\tau^2}{2\theta\Delta t}(\ddot{U}_{t+\theta\Delta t} - \ddot{U}_t) \tag{13}$$

$$U_{t+\tau} = U_t + \dot{U}_t\tau + \frac{1}{2}\ddot{U}_t\tau^2 + \frac{\tau^3}{6\theta\Delta t}(\ddot{U}_{t+\theta\Delta t} - \ddot{U}_t) \tag{14}$$

When $\tau = \theta\Delta t$, i.e:

$$\dot{U}_{t+\theta\Delta t} = \dot{U}_t + \frac{\theta\Delta t}{2}(\ddot{U}_{t+\theta\Delta t} + \ddot{U}_t) \tag{15}$$

$$U_{t+\theta\Delta t} = U_t + \theta\Delta t\dot{U}_t + \frac{\theta^2\Delta t^2}{6}(\ddot{U}_{t+\theta\Delta t} + 2\ddot{U}_t) \tag{16}$$

In this way, it can be sought:

$$\ddot{U}_{t+\theta\Delta t} = \frac{6}{\theta^2\Delta t^2}(U_{t+\theta\Delta t} - U_t) - \frac{6}{\theta\Delta t}\dot{U}_t - 2\ddot{U}_t \tag{17}$$

$$\dot{U}_{t+\theta\Delta t}=\frac{3}{\theta\Delta t}(U_{t+\theta\Delta t}-U_t)-2\dot{U}_t-\frac{\theta\Delta t}{2}\ddot{U}_t \tag{18}$$

At this point it is only necessary to consider the equilibrium equation (11) at the moment $t+\theta\Delta t$ to obtain the solutions for the displacement, velocity and acceleration at the moment $t+\Delta t$, noting that the projected load vector is linear, i.e.:

$$R_{t+\theta\Delta t}=R_t+\theta(R_{t+\Delta t}-R_t) \tag{19}$$

The specific calculation steps are:

Step1: Initial calculation

a/ Form the stiffness matrix K, mass matrix M and damping matrix C.

b/Calculate the initial U_0, $\dot{U}_0$, $\ddot{U}_0$.

c/ Pick the time step Δt. Calculate the coefficients: $a_0=\frac{6}{(\theta\Delta t)^2}$, $a_1=\frac{3}{\theta\Delta t}$, $a_2=2a_1$, $a_3=\frac{\theta\Delta t}{2}$, $a_4=\frac{a_0}{\theta}$, $a_5=\frac{-a_2}{\theta}$, $a_6=1-\frac{3}{\theta}$, $a_7=\frac{\Delta t}{2}$, $a_8=\frac{\Delta t^2}{6}$.

d/ forms the effective stiffness matrix:

$$\hat{K}=K+a_0M+a_1C \tag{20}$$

e/ for $\hat{K}$ as a triangular decomposition:

$$\hat{K}=LDL^T \tag{21}$$

Step2: Calculation within the time step

a/ Calculate the effective load at moment $t+\theta\Delta t$:

$$\begin{aligned}\hat{R}_{t+\theta\Delta t}=&R_t+\theta\left(R_{t+\Delta t}-R_t\right)\\&+M\left(a_0U_t+a_2\dot{U}_t+2\ddot{U}_t\right)+C\left(a_1U_t+2\dot{U}_t+a_3\ddot{U}_t\right)\end{aligned} \tag{22}$$

b/ Calculate the displacement at the moment $t+\theta\Delta t$:

$$LDL^TU_{t+\theta\Delta t}=\hat{R}_{t+\theta\Delta t} \tag{23}$$

c/ Calculate the displacement, velocity and acceleration at the moment $t+\theta\Delta t$:

$$\ddot{U}_{t+\Delta t}=a_4(U_{t+\theta\Delta t}-U_t)-a_5\dot{U}_t-a_6\ddot{U}_t \tag{24}$$

$$\dot{U}_{t+\Delta t}=\dot{U}_t+a_7(\ddot{U}_{t+\Delta t}+\ddot{U}_t) \tag{25}$$

$$U_{t+\Delta t}=U_t+\Delta t\dot{U}_t+a_8(\ddot{U}_{t+\Delta t}+2\ddot{U}_t) \tag{26}$$

(2) The Newmark integration format, also a generalization of the linear acceleration method, uses the following assumptions:

$$\dot{U}_{t+\Delta t}=\dot{U}_t+[(1-\delta)\ddot{U}_t+\delta\ddot{U}_{t+\Delta t}]\Delta t \tag{27}$$

$$U_{t+\Delta t}=U_t+\Delta t\dot{U}_t+\left[\left(\frac{1}{2}-a\right)\ddot{U}_t+a\ddot{U}_{t+\Delta t}\right]\Delta t^2 \tag{28}$$

The parameters a and δ are determined according to the accuracy and stability requirements of the integration, and Newmark originally proposed the “constant-mean-acceleration method” as the format for unconditional stabilization.

To obtain solutions for the displacement, velocity and acceleration at the moment $t+\Delta t$, it is only necessary to consider the equilibrium equations (11) for $t+\Delta t$, as follows:

Step1: Initial calculation

a/ Form the stiffness matrix K, mass matrix M and damping matrix C.

b/Calculate the initial U_0, $\dot{U}_0$, $\ddot{U}_0$.

c/ Pick the time step Δt, parameters a and δ. Calculate the integration coefficients: $\delta \geq 0.5$, $a \geq 0.25(0.5+\delta)^2$, $a_0 = \frac{1}{a\Delta t^2}$, $a_1 = \frac{\delta}{a\Delta t}$, $a_2 = \frac{1}{a\Delta t}$, $a_3 = \frac{1}{2a} - 1$, $a_4 = \frac{\delta}{a} - 1$, $a_5 = \frac{\Delta t}{2}\left(\frac{\delta}{a} - 2\right)$, $a_6 = \Delta t(1-\delta)$, $a_7 = \delta \Delta t$.

d/ forms the effective stiffness matrix:

$$\hat{K} = K + a_0 M + a_1 C \tag{29}$$

e/ for $\hat{K}$ as a triangular decomposition:

$$\hat{K} = LDL^T \tag{30}$$

Step2: Calculation within the time step

a/ Calculate the effective load at moment $t + \Delta t$:

$$\hat{R}_{t+\Delta t} = R_{t+\Delta t} + M(a_0 U_t + a_2 \dot{U}_t + a_3 \ddot{U}_t) + C(a_1 U_t + a_4 \dot{U}_t + a_5 \ddot{U}_t) \tag{31}$$

b/ Calculate the displacement at the moment $t + \Delta t$:

$$LDL^T U_{t+\Delta t} = \hat{R}_{t+\Delta t} \tag{32}$$

c/ Calculate the velocity and acceleration at the moment $t + \Delta t$:

$$\ddot{U}_{t+\Delta t} = a_0(U_{t+\Delta t} - U_t) - a_2 \dot{U}_t - a_3 \ddot{U}_t \tag{33}$$

$$\dot{U}_{t+\Delta t} = \dot{U}_t + a_6 \ddot{U}_t + a_7 \ddot{U}_{t+\Delta t} \tag{34}$$

When using the numerical integration method to analyze the seismic analysis of the structure, if the time increment Δt is greater than the self-oscillation period of the structural system by a number of times, the error will increase with the step-by-step integration, resulting in the dispersion of the calculation results without convergence. In summary, it is necessary to consider the influence of factors such as computational efficiency and computational accuracy, and to obtain a reasonable time increment step size based on experience or simplified simulation before analysis.

III. Seismic time-course analysis

Seismic time-varying analysis of a structure treats the structure as an elastic or elasto-plastic vibration system, loads the model with seismic acceleration, and then performs direct integration of the equations of motion to obtain the time-varying curves of the individual mass points in the system, and also to obtain the shear time-varying curves.

III. A. Modal analysis

When using ABAQUS for seismic time-range analysis of structures, damping coefficients should be defined in the plastic properties of the material properties in order to reflect the attenuation response of the structure in actual vibration.

In general, the analysis uses Rayleigh damping, i.e., stiffness matrix K, damping matrix C and mass matrix M, with the relation $C = \alpha M + \beta K$. The coefficient α in the equation is fully named Alphae and represents the mass damping coefficient, which affects the low frequencies of the vibration as long as they are present. The coefficient β, named Beta, represents the stiffness damping coefficient, which mainly affects the high frequency of vibration.

In ABAQUS, the coefficients α and β are user-defined, and the equations for solving the coefficients α and β are:

$$\begin{cases} 2 \times \xi \times \omega_1 = \alpha + \beta \times \omega_1^2 \\ 2 \times \xi \times \omega_2 = \alpha + \beta \times \omega_2^2 \end{cases} \tag{35}$$

where ξ is the damping ratio of the structure. ω_1 and ω_2 are the first and second order frequencies of the structural model, respectively.

III. B. Equations of motion

Structures in the seismic time course analysis, in order to facilitate the analysis and calculation, when the calculation meets the calculation accuracy required by the project, the actual structural system can generally be abstracted into a mass system to analyze.

If the mass of the structure is concentrated at one point, the structure can be simplified into a single mass point system. If the mass of the structure is more dispersed, the structure will be simplified into a multi-plasma point system when analyzing. From D'Alembert's theory, after derivation it can be concluded that the differential equation of motion of the multi-degree-of-freedom structural system, under seismic action in Eq:

$$[M]\{\ddot{x}\}+[C]\{\dot{x}\}+[K]\{x\}=[M]\{\ddot{x}_g\} \tag{36}$$

where $[M]$, $[C]$, $[K]$ are the mass matrix, damping matrix and stiffness matrix of the system, respectively. $\{\ddot{x}\}$, $\{\dot{x}\}$, $\{x\}$ are the acceleration vector, velocity vector, and displacement vector of the system, respectively. The $\{\ddot{x}_g\}$ is the acceleration vector of the seismic wave.

III. C. Seismic wave selection

Under current technological conditions, it is not possible to predict the occurrence of earthquakes with complete accuracy. However, dynamic time-range analysis can use seismic waves to simulate them. This method can both reproduce the seismic waveforms at the time of the earthquake and meet the needs of practical engineering. Since the occurrence of earthquakes is extremely complex and unpredictable, and the selection of seismic waveforms used is too homogeneous and will change with the change of site type, the selection of seismic waveforms is crucial for the time-course analysis of structures.

III. C. 1) Principles of seismic wave selection

(1) The selection of seismic waves should take into account the basic intensity of the area where the building is located and the site category, and should be made in accordance with the design seismic grouping. In order to ensure the accuracy of the analysis, real seismic records and artificially simulated acceleration time course curves should be selected, of which the number of real seismic records should not be less than two thirds of the total number. In addition, site characteristics, structure type, engineering structure, seismic intensity and other factors should be taken into account to comprehensively analyze the effects of seismic response and determine the most appropriate seismic response analysis results.

(2) The structural base shear at each moment can be obtained by calculating the structural base shear at each moment, which is superimposed by the results of multiple time-range curves, and the average value of which cannot be lower than 80%.

(3) The duration of seismic wave refers to the time span of vibration energy produced by seismic wave when it acts on the building structure. Normally, it should not be smaller than the basic self-oscillation period of the building structure which is 5 times and 15s, but it is only an average value. In reality, the self-oscillation period of the building structure will be different, so the duration of seismic wave will be different as well.

III. C. 2) Selection of seismic waves and calculation conditions

Two types of seismic waves are selected for time-range analysis, including El Centro horizontal seismic waves and Kumamoto 3D seismic waves in Kyushu, Japan.

The basic setup parameters of the horizontal and 3D seismic waves are shown in Table 1.

Table 1: The basic parameters of horizontal seismic wave and 3d seismic wave are set

Seismic wave	Direction	Acceleration peak	Time interval
El centro wave	N-S	345.04	0.02s
Three parts of Japan's nine states	E-W	1164.27	0.01s
	N-S	-744.01	
	U-D	875.62	

The analysis of 22 kinds of time-course analysis cases is shown in Table 2, and the elastic-plastic time-course analysis of the 5- and 10-story 3×3-span reinforced concrete space frame solid model under multiple and rare earthquakes is carried out according to the 22 kinds of cases in the table.

The elastic-plastic time-course analysis of seismic waves of the frame structure is calculated by using a high-performance server workstation, and each calculation case is 30 s. The 5-story frame requires 32 hours of calculation for each case, and the 10-story frame requires 45 hours of calculation for each case.

Table 2: 22 time range analysis

Operating condition	Layer number	Seismic wave name	Direction	Intensity of intensity	The acceleration peak (gal)	Remark
1	5	El centro wave	N-S	7 degrees	50	The frame reaches the limit state
2	5	El centro wave	N-S	8 degrees	100	
3	5	El centro wave	N-S	9 degrees	150	
4	5	El centro wave	N-S	Rare level 7	300	
5	5	El centro wave	N-S	Rare level 8	500	
6	5	El centro wave	N-S	Rare level 9	700	
7	5	El centro wave	N-S	0.9g	900	
8	5	El centro wave	N-S	1.2g	1200	
9	5	El centro wave	N-S	1.3g	1300	
10	5	El centro wave	N-S	1.5g	1500	
11	5	Three parts of Japan's nine states	E-W	Primordial	-1204.6	Failure
			N-S		-675.6	
			U-D		897.2	
12	10	El centro wave	N-S	7 degrees	50	The frame reaches the limit state
13	10	El centro wave	N-S	8 degrees	100	
14	10	El centro wave	N-S	9 degrees	150	
15	10	El centro wave	N-S	Rare level 7	300	
16	10	El centro wave	N-S	Rare level 8	500	
17	10	El centro wave	N-S	Rare level 9	700	
18	10	El centro wave	N-S	0.9g	900	
19	10	El centro wave	N-S	1.2g	1200	
20	10	El centro wave	N-S	1.3g	1300	
21	10	El centro wave	N-S	1.5g	1500	
22	10	Three parts of Japan's nine states	E-W	Primordial	-1204.6	Failure
			N-S		-675.6	
			U-D		897.2	

III. D. Modeling process for time-series analysis using ABAQUS

(1) ABAQUS/Explicit explicit solver was chosen for the seismic time-range analysis. The use of ABAQUS/Explicit solver can save computational cost to a great extent and save time as well as reduce disk and memory consumption when performing dynamic analysis of nonlinear problems.

(2) In the Load module, the seismic wave acceleration curve is applied to the bottom of the modeled structure as a boundary condition, i.e., it is equivalent to a seismic load acting on the foundation of the structure.

(3) Submit the Job task for analysis. In the post-processing module, the results of the time-range curves at the corresponding locations of the structural model can be extracted, and the performance of the structure against earthquakes can be analyzed by comparing the results of the individual curves.

III. E. Seismic performance comparison

The structural arrangement form of center support can be divided into single diagonal bar support (symmetrical arrangement), cross support, herringbone support or V-shaped support, K-shaped support, etc.. Among them, the symmetrically arranged single diagonal bar support and cross support are the support arrangement forms with the largest lateral stiffness and bearing capacity in the center support, and are most widely used when the height and width of the structure are close to each other.

In this paper, BEAM188 unit is selected for the simulation of beams, columns and supports. This cell supports creep and plasticity models (without considering the cross-section of the sub-model), and its cross-section can be composed of different materials, which makes it suitable for analyzing slender to moderately slender beam structures. Each BEAM188 cell contains a total of 2 nodes, defined by nodes I, J and K in the overall coordinate

system. The third order deformation assumption is used for the beam cells in the analysis and the neutral plane satisfies the flat section assumption.

For the floor slabs, SHELL181 finite-strain shell cells were selected, which are suitable for modeling thin to moderately thick shell structures. Each SHELL181 cell contains four nodes (I, J, K, and L nodes), and each node has six degrees of freedom. The cell can be used for layered structures by varying the thickness of the shell in nonlinear analysis. Its KEYOPT(3)=2 is set in the modeling analysis so that it has the same characteristics as the SHELL63 unit.

Considering that the cast-in-place concrete floor slabs in the light steel structure project are erected on the primary and secondary beams, i.e., the beam height does not include the thickness of the floor slab, the node bias options of the beams and floor slabs units are changed in ANSYS modeling, the primary and secondary beams units are inserted using TOP, and the floor slabs units are inserted using BOTTOM in order to meet the reality of the beams' upper part and the slab's lower part being flush, and the calculation results are more accurate, and in addition, columns, which are axial compression members, can not be used. In addition, the column is an axial compression member, so it can be inserted without offsetting, and the default center point can be used.

III. E. 1) Lateral Stiffness Comparison

The magnitude of lateral stiffness has a significant impact on the structural self-oscillation period and inter-story displacement angle, etc. In order to compare the lateral stiffness of the pure frame model and the four plus center braced frame models, a uniform load of size 10kN (to keep the structure in the elastic range) in the direction of Y-axis is applied to the top storey of each model by means of applying to the nodes in ANSYS and the top storey displacements are obtained after static analysis and the lateral stiffness is calculated.

The comparison of lateral stiffness of different forms of center braced frames is shown in Table 3. It can be seen that the lateral stiffness of the frame with herringbone bracing is the largest, and the lateral stiffness of the frame with cross bracing is slightly smaller than the former. This is followed by the V-shaped braced frame. The last is the symmetrically arranged single diagonal bar braced frame, but all of them have greater lateral stiffness than the pure frame, and all of them are more than two times of the lateral stiffness of the pure frame. The lateral stiffness of the braced frame with herringbone center reaches about 4 times of the lateral stiffness of the pure frame. Excluding the connection plate and bolts, the amount of steel used for bracing in descending order: KJX>KJM=KJV>KJI.

Table 3: The resistance stiffness comparison of different forms of frame

Model number	Top displacement(mm)	Compared to KJ	Lateral stiffness $\left(\times 10^6 N/m\right)$	Compared to KJ	No steel in the support of the connection (kg)
KJ	8.157	1	1.524	1	/
KJI	3.004	0.347	3.697	3.025	12236.641
KJX	2.146	0.269	4.965	4.119	25087.553
KJM	2.035	0.255	5.421	4.243	16931.229
KJV	2.473	0.304	4.423	3.708	15707.544

III. E. 2) Comparison of dynamic characteristics

Four frame models with center support are analyzed modally and the self-oscillating frequencies of the first 6 orders of modes of the structure are extracted. The first 6 orders of self-oscillation frequencies of each model are shown in Fig. 2, and Figs. (a) and (b) show the frequencies as well as the increasing terms of each model, respectively. Each increasing term is relative to the self-resonant frequency of the pure frame.

The increase in the self-oscillation frequency of the four center-supported frames compared to the pure frame in the first-order mode is basically the same, which is KJI=1.127, KJX=1.1553, KJM=1.1655, and KJV=1.1094, respectively, because the first-order vibration mode is longitudinal translational.

For the second order modes, the herringbone braced frame increases the frequency the most, the cross braced frame is slightly lesser followed by the V braced frame. And the symmetrically arranged single diagonal bar braced frame is the smallest with KJI = 0.8594.

The variation of third order self-oscillation frequency follows the same pattern. The frame with herringbone center support has the best integrity and has the largest increase in the self-oscillation frequency of the frame section.

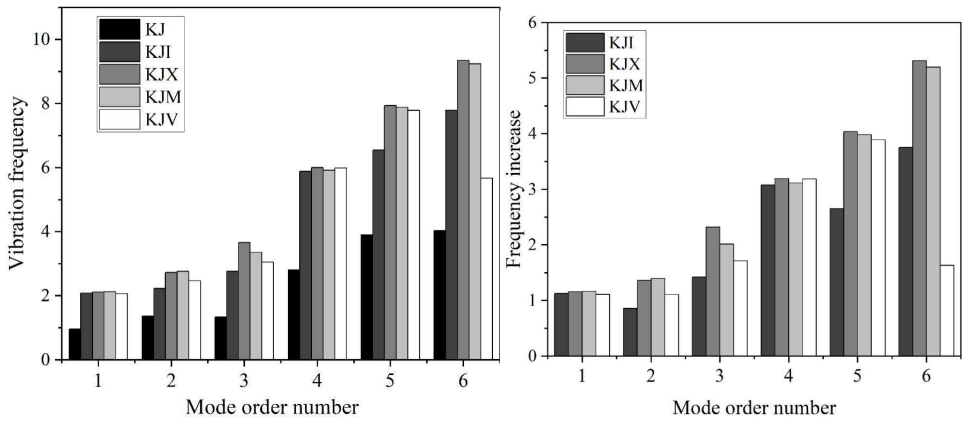

(a) frequency (b) Increase term

Figure 2: The first six order vibration frequency of each model

III. F. Time-Range Response Analysis

Here we analyze the absolute floor displacements and inter-story time response of the structural system for two types of frame structures with 5 and 10 floors under the action of rarefaction of 9 degrees (peak acceleration of 900 gal).

The maximum absolute floor displacements of the frame structures are shown in Fig. 3, and Figs. (a) and (b) show the absolute floor displacements of the 5-story and 10-story frames, respectively.

The absolute displacements of the floors show a tendency of repeated oscillations with time, and the waveforms of the floors are basically the same. The absolute displacements of the two frame floors increase with the increase of the floor number, showing an upward trend.

The range of absolute displacements of 5-floor framed floors in Fig. (a) is between -300 mm and 200 mm.

The absolute displacement range of 10-story frame floor in Fig. (b) is between -400mm~500mm.

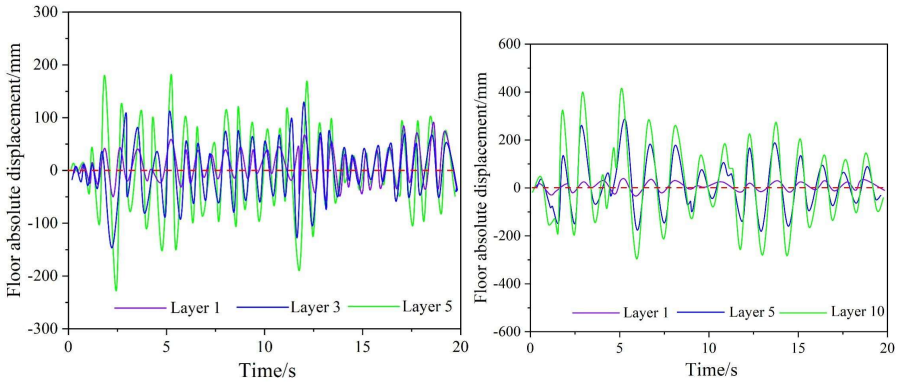

(a) 5 layer frame (b) 10 layer frame

Figure 3: Absolute displacement of the maximum floor of the frame structure

The maximum inter-story relative displacement and the inter-story displacement angle of the frame structure are shown in Fig. 4. The inter-story relative displacements of the floors show a tendency of repeated oscillations with time, and the waveforms are basically the same for all floors.

For the 5-story frame, the maximum inter-story relative displacement is at the ground floor. The inter-story displacement decreases with the increase of the floor number. The maximum inter-story displacement is about 76 mm.

For 10-story frames, the maximum interstory displacement is at the third story. And with the increase of the floor number, the interstory displacement first increases and then decreases, showing an inverted triangle trend, and the maximum interstory displacement is in the range of 55mm~60mm.

After 900 gal seismic wave, the maximum interstory displacement angle of 5 and 10-story frame structure is about 0.017 and 0.015, respectively, and both of them are smaller than the plastic interstory displacement angle limit value

of 0.02, which indicates that both frames have good lateral displacement resistance and stiffness, and have good seismic performance.

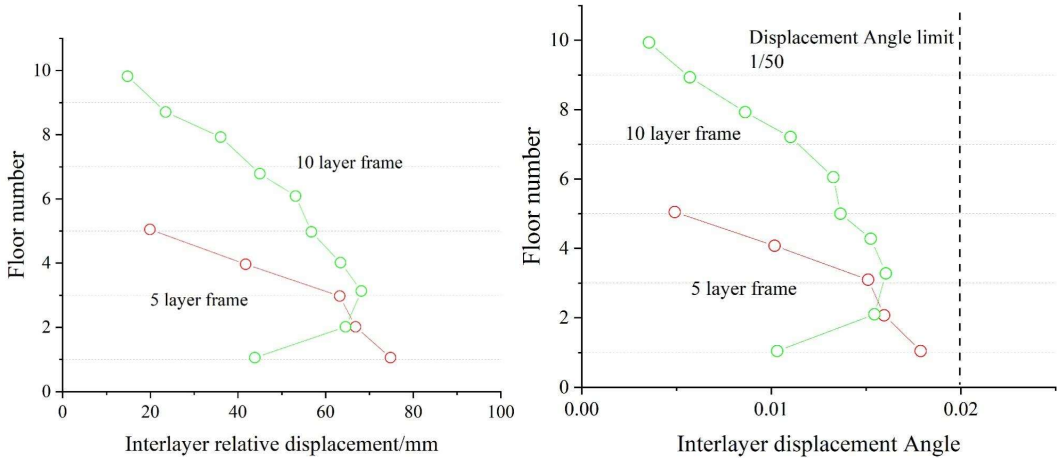

(a) Interlayer relative displacement (b) Interlayer displacement Angle

Figure 4: Relative displacement and interlayer displacement Angle

IV. Conclusion

Reinforced concrete frame structures with different bracing forms show significant differences under seismic action. The results of time-course analysis show that the frame with herringbone bracing has the best performance in terms of lateral stiffness, which is 4 times that of the pure frame; followed by the frame with cross bracing and the V-braced frame, which are 2.6 and 2.3 times that of the pure frame, respectively. For the 5-story frame, the maximum floor displacements were from -300 mm to 200 mm, and the maximum inter-story displacements were 76 mm; for the 10-story frame, the maximum floor displacements were from -400 mm to 500 mm, and the maximum inter-story displacements were 60 mm, which indicate that the structure showed good seismic performance under different bracing forms. The analysis shows that the frame structure with center bracing can effectively improve the lateral displacement resistance and stiffness of the structure in the face of large earthquakes, showing stronger seismic performance. In addition, all the analyzed results show that all types of bracing forms have a significant role in improving the seismic performance of frame structures.

References

[1] Karadag, O., & Canakcioglu, N. G. (2024). Teaching earthquake-resistant structural systems in architecture department: a hands-on learning experience. Architectural Science Review, 67(4), 332-344.

[2] Morales-Beltran, M., & Yildiz, B. (2020). Integrating configuration-based seismic design principles into architectural education: teaching strategies for lecture courses. Architectural Engineering and Design Management, 16(4), 310-328.

[3] Turgeon, B. (2014). Designing Earthquake-Resistant Structures: Integrating Science and Engineering Practices. Science Scope, 38(3), 49-57.

[4] Mwangi, J. P. (2013, June). Teaching Building Professionals Design of Earthquake Resistant Buildings: Haiti Experience. In 2013 ASEE Annual Conference & Exposition (pp. 23-1138).

[5] Zakian, P., & Kaveh, A. (2023). Seismic design optimization of engineering structures: a comprehensive review. Acta Mechanica, 234(4), 1305-1330.

[6] Uang, C. M., & Bruneau, M. (2018). State-of-the-art review on seismic design of steel structures. Journal of Structural Engineering, 144(4), 03118002.

[7] Solís, M., Romero, A., & Galvín, P. (2012). Teaching structural analysis through design, building, and testing. Journal of Professional Issues in Engineering Education and Practice, 138(3), 246-253.

[8] Pereiro-Barceló, J., Bonet, J. L., Gisbert-Doménech, C. M., & Valiente-Sanz, R. (2018). TEACHING-LEARNING METHODOLOGY, ASSESSMENT AND RESULTS OF THE “SEISMIC DESIGN OF STRUCTURES” SUBJECT OF SECOND COURSE OF SPECIALIZED MASTER IN CIVIL ENGINEERING AT UNIVERSITAT POLITÈCNICA DE VALÈNCIA. In INTED2018 Proceedings (pp. 6526-6530). IATED

[9] English, L. D., King, D., & Smeed, J. (2017). Advancing integrated STEM learning through engineering design: Sixth-grade students’ design and construction of earthquake resistant buildings. The Journal of Educational Research, 110(3), 255-271.

[10] Morales-Beltran, M., Charleson, A., & Aydin, E. E. (2020). Sawtooth method for teaching seismic design principles to architecture students. Journal of Architectural Engineering, 26(1), 04019031.

[11] Arabacıoğlu, F. P., Er, İ. E., & Tastan, H. (2025). The investigation into the relationship between seismic design and architectural education: a systematic literature review. Journal of Asian Architecture and Building Engineering, 1-26.

[12] Jagota, V., Sethi, A. P. S., & Kumar, K. (2013). Finite element method: an overview. Walailak Journal of Science and Technology (WJST), 10(1), 1-8.

[13] Erhunmwun, I. D., & Ikponmwosa, U. B. (2017). Review on finite element method. Journal of Applied Sciences and Environmental Management, 21(5), 999-1002.
[14] Sabat, L., & Kundu, C. K. (2020). History of finite element method: a review. Recent Developments in Sustainable Infrastructure: Select Proceedings of ICRDSI 2019, 395-404.
[15] Wang, S., Wang, X., & Peng, F. (2023, April). Application of finite element method in engineering mechanics teaching. In Proceedings of the 9th International Conference on Education and Training Technologies (pp. 1-6).
[16] Guo, Y., Yang, L., Chen, X., & Yang, L. (2020). An engineering-problem-based short experiment project on finite element method for undergraduate students. Education Sciences, 10(2), 45.
[17] Xuanyu Ge,Linglong Zhou,Sara Bagherifard & Mario Guagliano. (2025). A simple and efficient implementation of explicit phase field method in ABAQUS to address complex three-dimensional fracture problems. Engineering Fracture Mechanics,323,111222-111222.
[18] Xue Chun Liu,Wen Bin Cui,Xuesen Chen & Long Xin Guo. (2025). Seismic performance of a post-earthquake repair-free bolted beam-to-column joint with slab. Engineering Structures,337,120491-120491.